25th ABCM International Congress of Mechanical Engineering
October 20-25, 2019, Uberlândia, MG, Brazil

COB-2019-0759
STELLAR VARIABILITY MODELING FOR AUTONOMOUS STAR TRACKER SIMULATOR

Luis Henrique Inagaki da Silva
Fábio de Oliveira Fialho
Polytechnic School of the University of São Paulo, 05508-010 - São Paulo, SP, Brazil
luis.inagaki@usp.br / fabio.fialho@usp.br

Abstract. *Star trackers are key sensors in high accuracy Attitude Control Systems (ACS) for satellites. They are 3-axis orientation sensors composed of a telescope and an electronic camera. In order to develop a star tracker, simulators of various subsystems are required. Among them, the image formation simulator stands out. It simulates the complete process of creating a digital image. Star trackers rely on stars positions to derive the satellite orientation, but stars are not steady objects. They evolve provoking from time to time considerable variation in their light emission. Such a stellar variability provokes inaccuracies in the satellite Line-of-Sight (LoS) calculation since brightness variation influences the calculation of star centroids, the very basic information used to derive the LoS.*
This paper aims to characterize the stellar variability, modeling and including them in an image formation simulator in order to design a robust star tracker flight software, mitigating losses of accuracy of the satellite orientation measurement. The methodology consists of determining the most common astrophysical phenomena in observable stars reachable by star trackers. To know what type of stellar variability is relevant, we use a star catalogue. Then, we create simplified models for them. Approximately, 2,900 over 21,000 stars with apparent magnitude $\boldsymbol{m_V \leq 7}$ *have relevant brightness variation in their light curves. Therefore, they impact the performance of LoS calculation. The developed algorithms and tools allow for simulating several stellar phenomena in the same light curve. The modeling method is adequate to avoid unnecessary complexity regarding star tracker flight software development.*

Keywords: *Satellite, Attitude Control System, Autonomous Star Tracker, Stellar Variability, Image Formation Simulator.*

1. INTRODUCTION

In May 2012, the Brazilian Federal Government approved the **Strategic Program for Space Systems** (PESE) via the Administrative Rule No. 224 / GC3. PESE has been prepared by the Ministry of Defense, through the Aeronautical Command. Its content concerns the desires for the next decades of the three military forces in terms of satellites and their functionalities applied to national defense.

The development of critical technologies is required to cover PESE`s demands. One of them is the **Attitude and Orbit Control System** (*AOCS*), which is responsible for keeping the satellite **orientation** (*attitude*) and **position** (*orbit*) controlled with relation to an inertial frame. To perform this task, the satellite must be equipped with sensors and actuators working together to maintain it stable. Figure 1 shows a simplified block diagram of the **Attitude Control System** (*ACS*).

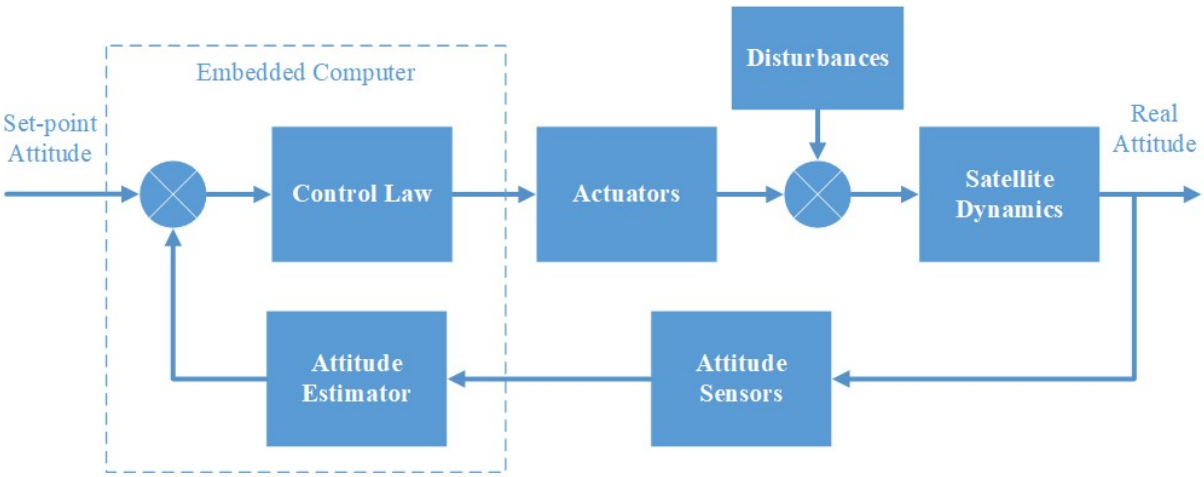

Figure 1 – Simplified ACS block diagram.

The control loop showed in Figure 1 requires attitude sensors. There are several types of off-the-shelf sensors in the market, like autonomous star trackers, solar sensors, magnetometers, and horizon sensors. Among them, only the autonomous star tracker has enough accuracy to reach the requirements established by PESE, for most of the required satellites.

The star tracker is an optoelectronic device that measures the 3-axis satellite attitude through stellar observations. It consists of a detector, a processing electronics, and a telescope. The detector collects photons from the observed stars converting them into electrical signals to form the image. The processing unit can perform star identification using a stellar catalog embedded and stored in firmware. Therefore, the attitude can be calculated autonomously by the sensor.

In order to develop a star tracker, simulators of various subsystems are required. Among them, the image formation simulator stands out. It simulates the complete process of creating a digital image, from the emission of light by the stars, going through the optical system, the conversion of photons into electrons by the detector, until the digitalization and storage of digital images from an observed scene. The image formation simulator is indispensable to the star tracker flight software development.

The image formation simulator consists of several algorithms. One of them is the stellar variability that is treated here. Stars are not steady objects. Many of them evolve provoking considerable variation in their light emission. They are called variable stars. Such a stellar variability provokes inaccuracies in the satellite Line-of-Sight (LoS) calculation, once brightness variation influences the calculation of star centroids, the very basic information used to derive the LoS.

In this way, it is important to understand such phenomena and characterize them, so that it is possible to include them in the image formation simulator in order to design a robust star tracker flight software, mitigating losses of accuracy of the satellite orientation measurement.

This paper is organized as follows: Section 2 presents an overview of star trackers. Section 3 describes our image formation simulator. Section 4 establishes the relationship between stellar variability and attitude determination. Section 5 deals with methodology and results. Finally, Section 6 presents discussions and conclusions.

2. STAR TRACKER

Star trackers are widely used in spacecraft that requires high accuracy in determining its attitude (on the order of arcseconds [(1)]). They have many advantages: low power consumption, absence of moving parts (increasing reliability and service life), ability to work in different operating modes allowing the same sensor to be used in different missions or different phases of the same mission, very small size and weight, stability, low irregularities in measurements (the opposite of those present in the Earth's magnetic field that influence magnetometers or drifts that are inherent to gyroscopes, for instance), among others. In the literature, star trackers are classified into two basic types:

- **Non-Autonomous Star Tracker:** This type of sensor does not process the image. Thus, it depends on an external processing unit to calculate the coordinates of the observed stars. This calculation can be done both in the satellite platform processor and on the ground.
- **Autonomous Star Tracker:** This type of sensor, besides processing the image, also determines its attitude, by identifying the coordinates of observed stars in an inertial frame. Such identification is obtained by comparison with a catalogue of stars stored in the star tracker itself.

Figure 2 shows a sketch of a star tracker and its basic parts.

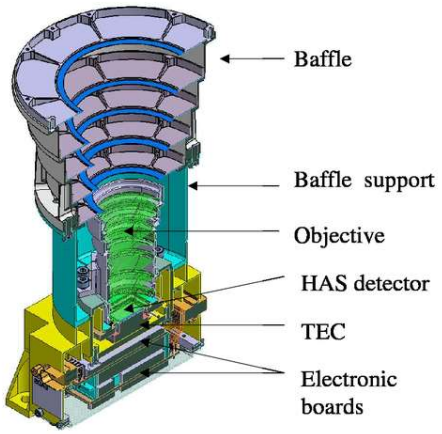

Figure 2 - Sketch of a star tracker[2].

[(1)] Unit of angular measurement, one arc second is equal to 1/3600 degrees.
[(2)] Source: https://www.spiedigitallibrary.org/ContentImages/Proceedings/10566/105660T/FigureImages/00021_PSISDG10566_105660T_page_3_1.jpg.

We identify in Figure 2 the baffle, responsible for filtering contaminant light, the lenses from the objective that compose the telescope, the CCD (Charge-Coupled Device) detector and the header tray where we can mount the front-end electronics and the processing data unit.

Figure 3 shows a sketch of the physical process of acquiring stellar images with star trackers.

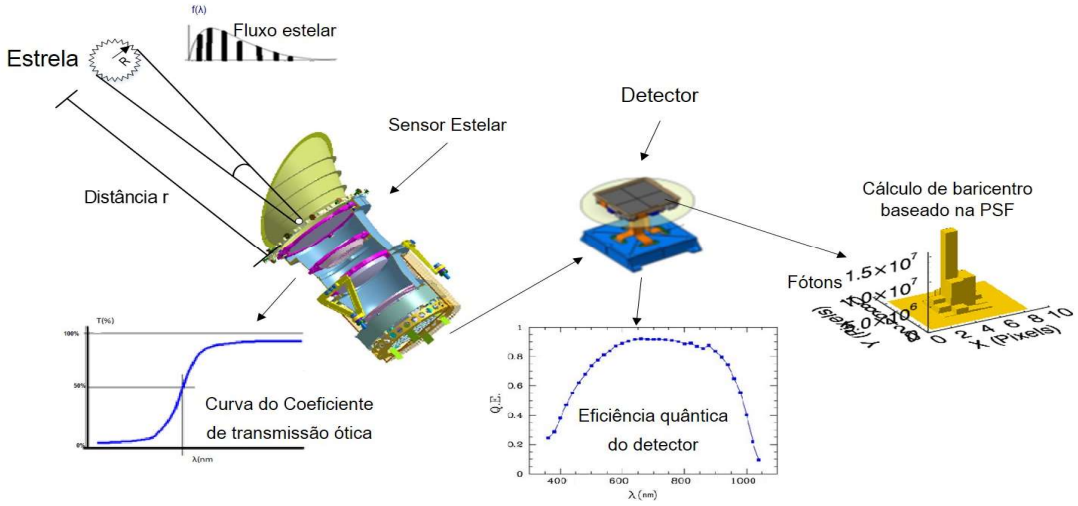

Figure 3 – Path of light through the sensor, from the star to the digital image.

1) The light emitted by stars is scattered in space, eventually reaching the star tracker. The undesirable light outside the sensor's FoV is filtered by the baffle.

2) After baffle filtering, the flux from stars passes through the optical system. This system has an optical transmission coefficient that indicates, in percentage, how much of the light coming in will cross it as a function of the wavelength.

3) The same optical system can be described by a **Point Spread Function** (*PSF*) which is nothing more than the convolution of a light source point by the optical response.

4) The spots are then formed in the detector for each star observed in the FoV.

5) The image is acquired during a certain time interval, which is called exposure time, which determines the number of photons that will be collected by the detector. The exposure time must be a compromise regarding the threshold of detectable stars and pixels saturation. The detector quantum efficiency also plays a role in how many photons will be converted into electrons.

6) After digitalization, the image containing the observed star can be processed by the flight software.

2.1 Star tracker operation

An autonomous star tracker typically operates in two modes:

- Initial attitude acquisition ("*LOST IN SPACE*");
- And tracking mode.

The difference between them is basically the role that each one plays and if an approximate knowledge of the attitude is available or not (Liebe, 2002).

The first mode is to perform the attitude determination without any initial information *("LOST IN SPACE*"). This function is based on a star pattern identification, which consists of comparing the information from an embedded star catalog with the stars detected in the FoV, deducing from it the LoS.

The second mode - normal mode of operation - assumes that the current attitude is close to the last estimated one. Thus, the window where the star is likely to be contained is estimated as well. The pixels in this window are processed and the centroid is calculated on them.

In both modes, LoS is sent to the AOCS via the military standard interface 1553[(3)], typically.

3. IMAGE FORMATION SIMULATOR

[(3)] Communication protocol and data bus in space vehicles created by the Department of Defense of the United States.

The **Image Formation Simulator** (*IFS*) is an application developed in **MATLAB** using the **APPDESIGN** tool. It aims to simulate all the star tracker image acquisition process, from the observed scenes in the FoV, passing through the optical system, photoelectron conversion by the detector, digitalization, and storage of digital images.

Furthermore, it simulates phenomena that happen during a mission that decrease the star tracker performance, like stellar activity, sky background, and variation of the position of stars due to detector nonlinearities.

Thus, IFS is a **Software Ground Support Equipment** (*SGSE*) essential to the star tracker flight software development. Figure 4 illustrates the blocks required to build an initial version of the IFS. The present work has implemented all the blocks of Figure 4 based on previous works from our team (Gennaro *et al.* 2016 and Burger *et al.* 2018) and the stellar variability development described in Section 5.

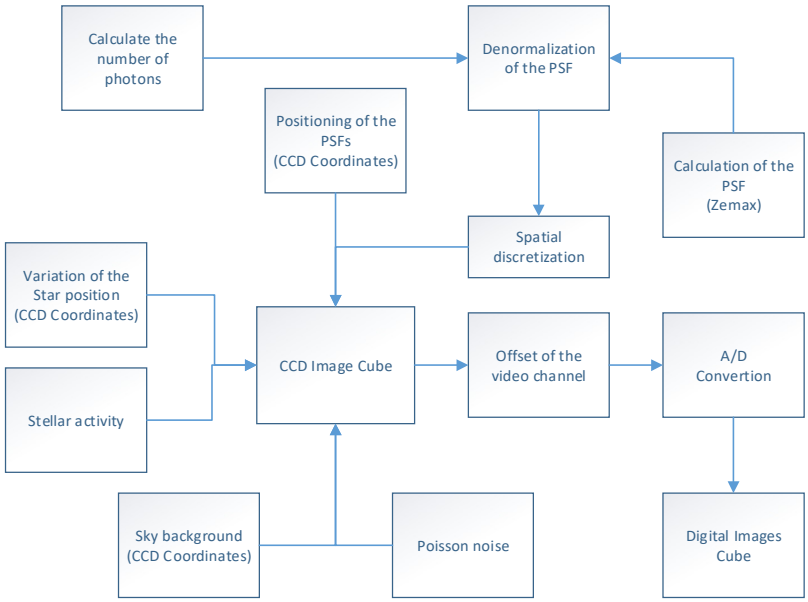

Figure 4 – IFS block diagram.

Each block can be explained as follows:

- **CALCULATION OF THE NUMBER OF PHOTONS:** It consists in providing an estimate of the number of photons (or electrons) collected by the detector from general astrophysical parameters of stars (apparent magnitude and effective temperature) and the star tracker itself according to Di Gennaro *et al.* (2016).
- **PSF CALCULATION**: Light passing through an optical system causes its dispersion on the detector. This dispersion can be represented by a normalized and discrete PSF. In our case, the Gaussian function is used as a first approximation. Zemax PSFs will be produced soon.
- **PSF DENORMALIZATION**: This step performs the multiplication of the number of photons by the PSF, resulting in a PSF with amplitude based on the observed star.
- **SPATIAL DISCRETIZATION**: Here the denormalized PSF is discretized based on the spatial resolution of the detector.
- **PSFs POSITIONING**: From the star catalog, the position of the star on the celestial sphere is projected on the detector and the PSF is positioned there.
- **VARIATION OF THE STARS POSITION**: Assuming a certain satellite dynamics and attitude control, the dynamic angular position error is propagated into the detector, generating spatial motion of stars with relation to the detector frame.
- **STELLAR ACTIVITY**: This box consists of the algorithms that simulate the astrophysical phenomena presented in the stellar variability section of this paper (Section 5).
- **SKY BACKGROUND**: During image acquisitions, the observed star is polluted by different sources of energy, such as the zodiacal light or the terrestrial albedo. It is necessary to simulate these sources of polluting light, which will be done in this block.
- **POISSON NOISE**: Noise inherent to the photon count made by the detector. It is simulated by a Poisson distribution noise at each pixel.
- **CCD IMAGE CUBE**: These are the resultant images over time of the entire process described so far, i.e., excluding the front-end electronics in charge of reading and digitalizing images.

- **VIDEO CHANNEL OFFSET**: This block implements voltage amplification and the preamplification offset of the image readout channel. Such an offset is intended to eliminate negative values in the processing unit since they have no physical meaning.
- **A/D CONVERTER**: Step needed to transform an analog signal into a digital signal, which consists of transforming the information collected by the detector into data that a computer can process and interpret.
- **CUBE OF DIGITAL IMAGES**: Here, the entire stage for the formation of the digital image is finished. It is this cube that will be later used as input data for the flight software simulator.

4. STELLAR VARIABILITY AND ATTITUDE DETERMINATION

4.1 Stellar variability

Variable stars can be classified into two main groups: intrinsic variables, in which physical changes occur in the star, that is, internal processes due to their physical and chemical properties; and extrinsic variables, in which changes occur because of external factors that influence the observed brightness of the star.

Intrinsic variables are classified in subclasses: pulsating variables, where stars show periodic expansion and contraction of their surface layers; eruptive variables, where stars vary in brightness because of violent processes and flares occurring in the chromosphere (a thin, hot layer just above the visible photosphere); and cataclysmic variables.

Apparent variability in the brightness of extrinsic stars is a perspective effect such as eclipsing binary, which is a system composed by two stars orbiting around the system center of mass, and rotating stars, whose have a non-uniform surface brightness and/or ellipsoidal shapes (not a perfect sphere).

4.2 Stellar variability influence over LoS calculation

Attitude determination refers to determining the spacecraft attitude based on two or more LoS measurements from an image. The attitude of a body is quantified by some rotation from the body frame with respect to an inertial frame. To perform the attitude determination there are several approaches, being TRIAC and QUEST the two most common ones (Warier et al., 2016). In the case of star trackers, one of the main inputs of the attitude estimation algorithm are the coordinates of the observed stars in the detector frame. The first step to obtain these inputs is to determine the centroids of the observed stars. Such measurements are performed inside star windows, which are small windows containing the guide stars. In those windows, a centroiding algorithm is used to accurately determine the centroids of stars (bar_{x_l}, bar_{y_l}) in the detector.

$$bar_{x_l}(k) = \frac{\sum_{j=1}^{n}\sum_{i=1}^{m}(\bar{N}_{e-}(i,j).i)}{\sum_{j=1}^{n}\sum_{i=1}^{m}(\bar{N}_{e-}(i,j))},\ bar_{y_l}(k) = \frac{\sum_{j=1}^{n}\sum_{i=1}^{m}(\bar{N}_{e-}(i,j).j)}{\sum_{j=1}^{n}\sum_{i=1}^{m}(\bar{N}_{e-}(i,j))} \tag{1}$$

where $\bar{N}_{e-}(i,j)$ is the mean number of electrons in pixel (i,j) and n and m are the dimensions of windows containing the stars.

The stellar variability influences centroid computation, hence, propagating it to the LoS calculation, which, in turn, generates inaccurate information for the ACS. Figure 5 shows an example of a binary eclipsing star and its influence on the centroid measurements.

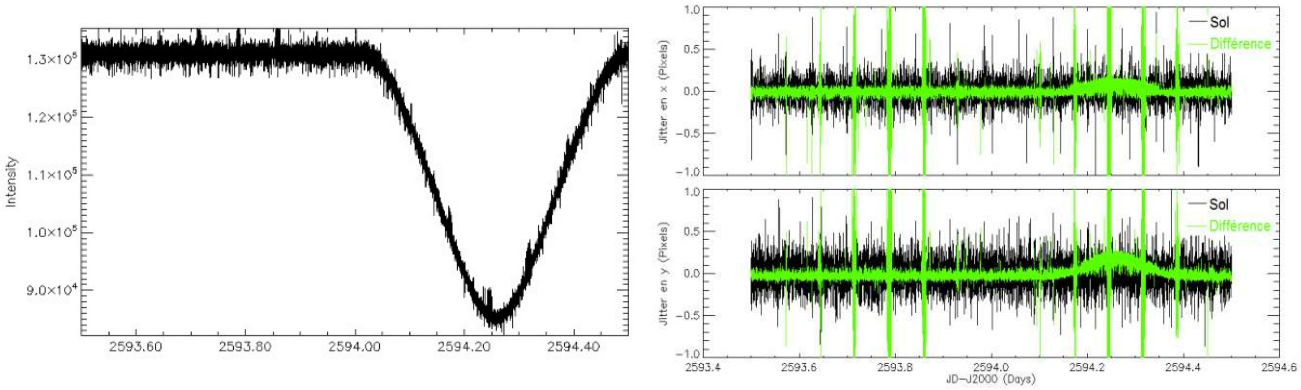

Figure 5 – In-orbit CoRoT satellite data showing the influence of stellar variability on centroid measurement. On the left the observed photometry of a binary system. On the right in black the centroid curves of a guide star rebuilt at high precision on the ground and the difference between them and on-board centroid measurement in green.

Green curves of the right plot show a loss of accuracy around 2594.2 Julian Days which is due to the drop in light flux coming from the star since Equation (1) depends on $\bar{N}_{e\_}(i,j)$, which varies over time.

This variation in the light curve consists of a significant variation of luminosity, to which the sensor is exposed. According to the phenomenon linked to the observed stars, different types of light curves are generated, provoking LoS inaccuracies. Therefore, it is important to simulate them in order to evaluate the robustness of the star tracker flight software.

5. METHODOLOGY AND RESULTS

The methodology consists of determining the most common astrophysical phenomena in observable stars reachable by star trackers. We assume an apparent magnitude 7 as a reasonable threshold for detectable stars. Then, we create simplified models for these phenomena and write algorithms to implement them in the image formation simulator. Therefore, in general, the approach chosen consists of algorithms composed by mathematical equations with configurable parameters, allowing users to simulate stellar variability that they deem necessary to develop and test the star tracker software.

5.1 Stellar variability distribution

To obtain the stellar variability distribution, a database server (*MARIADB*) containing Gaia [4] (Gaia Collaboration, 2018) and GCVS [5] (Samus N.N., 2017) catalogues was created as well as auxiliary algorithms for data manipulation in **MATLAB**. As a result, the most statistically relevant phenomena have been defined, which are Eclipsing Binary Systems, Pulsating Variable Stars, Eruptive Variable Stars, Cataclysmic (*Explosive or Nova-like*) Variables and Rotating Variable Stars. They represent about 87% of 3,338 cataloged stars [6] up to magnitude 7 (Figure 6).

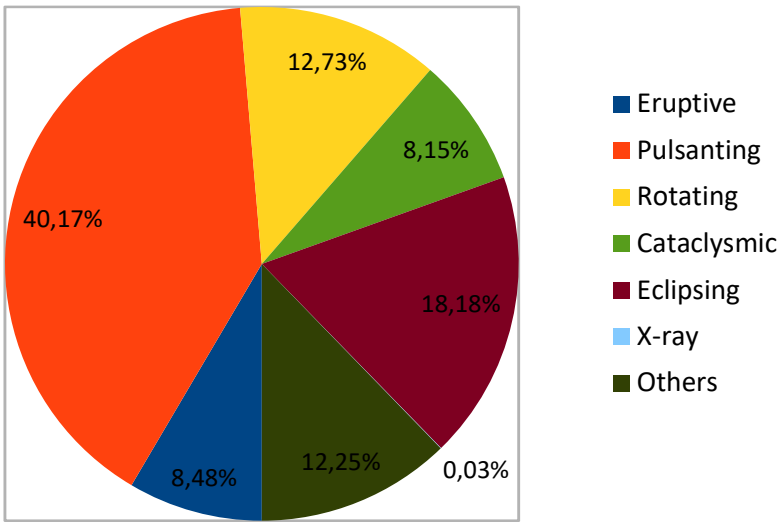

Figure 6- Stellar variability distribution for $m_V \leq 7$.

Their significant brightness variation could impact the LoS calculation. Therefore, they must be modeled and evaluated in the star tracker simulation software.

Examples of typical light curves for different types of variability are shown in Figure 7 (Vasily Belokurov, 2003).

[4] Gaia is a satellite of the European Space Agency (ESA) designed for astrometry: measuring position and distance of stars with a precision never reached before. The mission has been launched in 2013 and will help to build the largest and most accurate star catalog ever.

[5] GCVS (General Catalogue of Variable Stars) is the only reference source in all known variable stars. Its content has been published by researchers of variable stars in Moscow since 1946.

[6] There are about 21,000 stars up to magnitude 7 according the Gaia catalogue, but only 3,338 are classified in the GCVS catalogue.

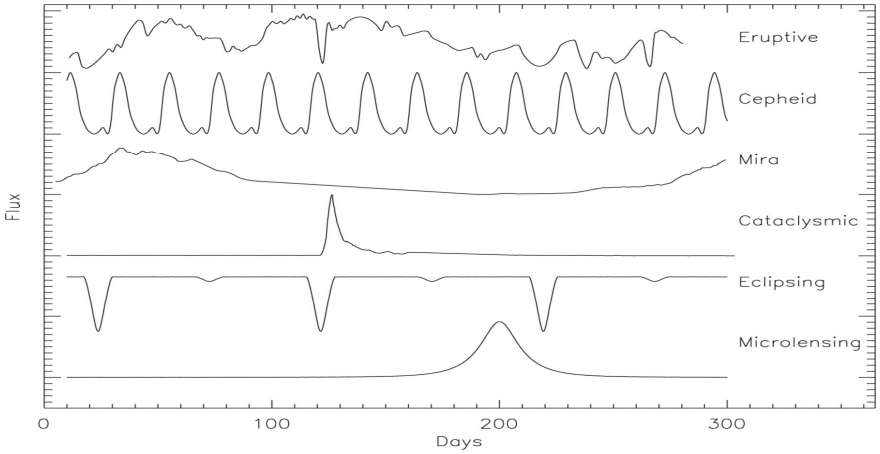

Figure 7 - Typical light curves for different types of variable stars.

5.2 Stellar variability Modeling

In this section, we present the algorithms developed to simulate the more relevant stellar phenomena presented in Figure 7. To simulate them and to avoid too much complexity using dynamic stellar modeling, the method of curve fitting has been applied to light curves of some observed stars to find out their approximated mathematical equations.

5.2.1 Stellar activity

Stellar activity is an astrophysical phenomenon related to the stellar magnetic field that induces light emission variations. In Sun-like stars, the magnetic field induces coronal mass ejection, flares, and sunspots, which occur at time scales from hours up to days. Meanwhile, stellar magnetic field cycles are observed in a decade time scale. As an example, the Sun has an 11-year magnetic field cycle while its short scale stellar activity is up to 5 days. Depending on the satellite life cycle, short or long periods will be more relevant with relation to each other regarding the star tracker.

For the stellar activity algorithm, data from the SOHO observatory, which is the reference for solar activity study, have been used. From a text file containing the Solar flux time series of short time scales, data can be read and visualized in the IFS Human-Machine Interface (HMI). It also allows users to modify the amplitude of the curve. Figure 8 shows a plot of SOHO data used in the simulator.

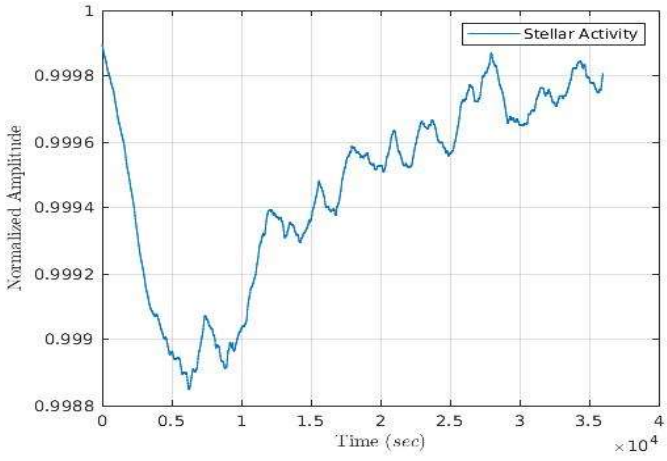

Figure 8 – Normalized in-orbit light curve from the SOHO space mission.

5.2.2 Flare

A solar flare is a sudden flash of light on the Sun, usually observed near its surface and close to a sunspot group. The magnetic field lines near the sunspots often tangle, cross, and reorganize themselves. This can cause an explosion of energy and release a lot of radiation into space. Flares are often, but not always, accompanied by a coronal mass ejection. Figure 9 shows an example of a light curve of a flare of an Eruptive Variable Star and its fitted curve.

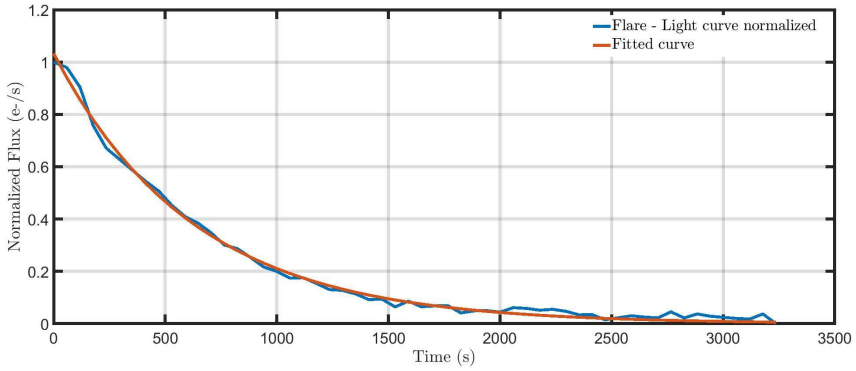

Figure 9 - Observed light curve for a flare and its fitted curve.

The corresponding fitted equation is of the form:

$$f(a,\tau,t) = ae^{(-\tau.t)} \tag{2}$$

where a is the flare amplitude, τ is the flare decay constant and t is time. These parameters are set up in the simulator interface.

5.2.3 Stellar oscillation

The stellar oscillations can be classified into two main categories: the pulsating variables and the cataclysmic variables. This classification is based mainly on profiles of behavior in the appearance of light curves, or the evolution of their spectral characteristics. Thus, the stars that present oscillations in their light curves are not in hydrostatic equilibrium since the forces are not counterbalanced and local accelerations cause the motion of the fluids. Figure 10 shows an example of a light curve of stellar oscillation and its fitted curve.

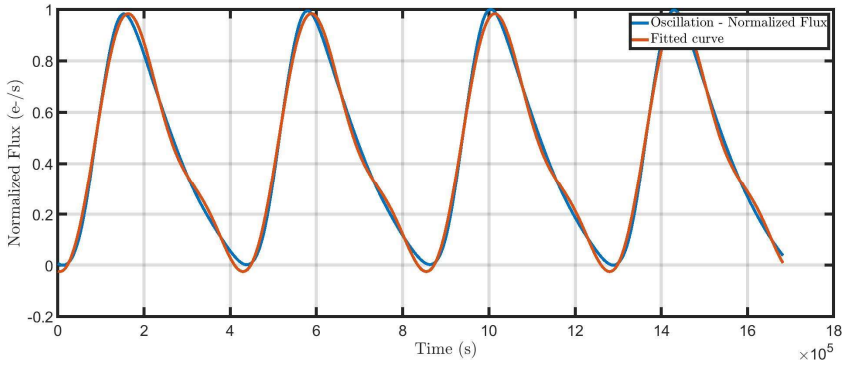

Figure 10- Observed light curve for stellar oscillations and its fitted curve.

The corresponding fitted equation is of the form

$$f(a_1,b_1,a_2,b_2,\omega,t) = a_1 cos(\omega t) + b_1 sin(\omega t) + a_2 cos(2\omega t) + b_2 \sin(2\omega t) \tag{3}$$

where $a1, b1, a2, and\ b2$ defines the overall amplitude of the oscillations, ω is the fundamental frequency of oscillations and t is time. These parameters are set up in the simulator interface.

5.2.4 Planetary transits

A planetary transit is a phenomenon where a planet passes between a star and the observer. From the observer perspective, the transiting body appears to move across the surface of the larger body, covering a small portion of it, and provoking, therefore, a slight drop in the measured flux. Figure 11 shows an example of a light curve of planetary transit and its fitted curve.

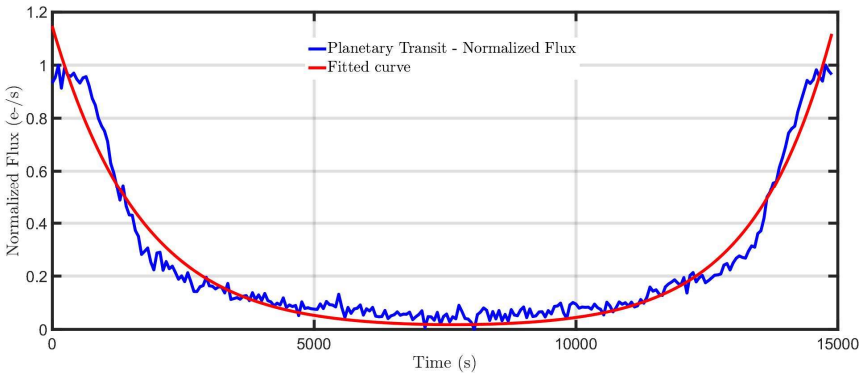

Figure 11 - Observed light curve for a planetary transit and its fitted curve.

The corresponding fitted equation is of the form

$$f(a_1, b_1, a_2, b_2, c_1, c_2, t) = a_1 e^{\left(\frac{-(t-b_1)}{c_1}\right)^2} + a_2 e^{\left(\frac{-(t-b_2)}{c_2}\right)^2} \quad (4)$$

where a_1, and a_2 define the transit depth, b_1, b_2, c_1, and c_2 define the transit width and t is time. The ensemble of parameters defines the transit shape. These parameters are set up in the simulator interface.

5.2.5 Binary transits

A binary system is a stellar system consisting of two stars orbiting their common center of gravity. Like planetary transits, observers will perceive periodic occultations in the light curve with shapes slightly different from planetary ones. More than half of visible stars are multiple star systems. Figure 12 shows an example of a light curve of a binary transit and its fitted curve.

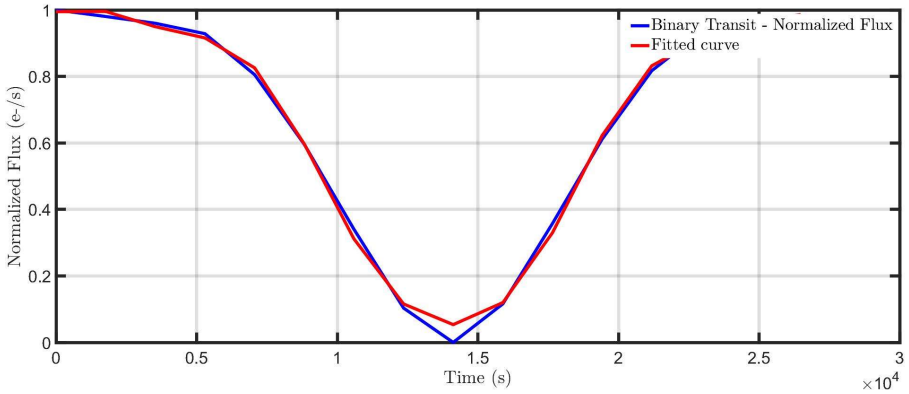

Figure 12 - Observed light curve of binary transit and its fitted curve.

The corresponding fitted equation is of the form

$$f(a_1, a_2, a_3, a_4, b_1, b_2, b_3, b_4, c_1, c_2, c_3, c_4, t) = a_1 e^{\left(\frac{-(t-b_1)}{c_1}\right)^2} + a_2 e^{\left(\frac{-(t-b_2)}{c_2}\right)^2} + a_3 e^{\left(\frac{-(t-b_3)}{c_3}\right)^2} + a_4 e^{\left(\frac{-(t-b_4)}{c_4}\right)^2} \quad (5)$$

where a_1, a_2, a_3, and a_4 define the transit depth, $b_1, b_2, b_3, b_4, c_1, c_2, c_3$, and c_4 define the transit width and t is time. The ensemble of parameters defines the transit shape. These parameters are set up in the simulator interface.

5.2.6 Stellar variability and the IFS user interface

As an overall result example, through an HMI, users can generate synthetic data of each phenomenon, which in the end will be summed up, resulting in a single light curve, representing the main characteristics of a real curve that would be observed by the star tracker (Figure 13).

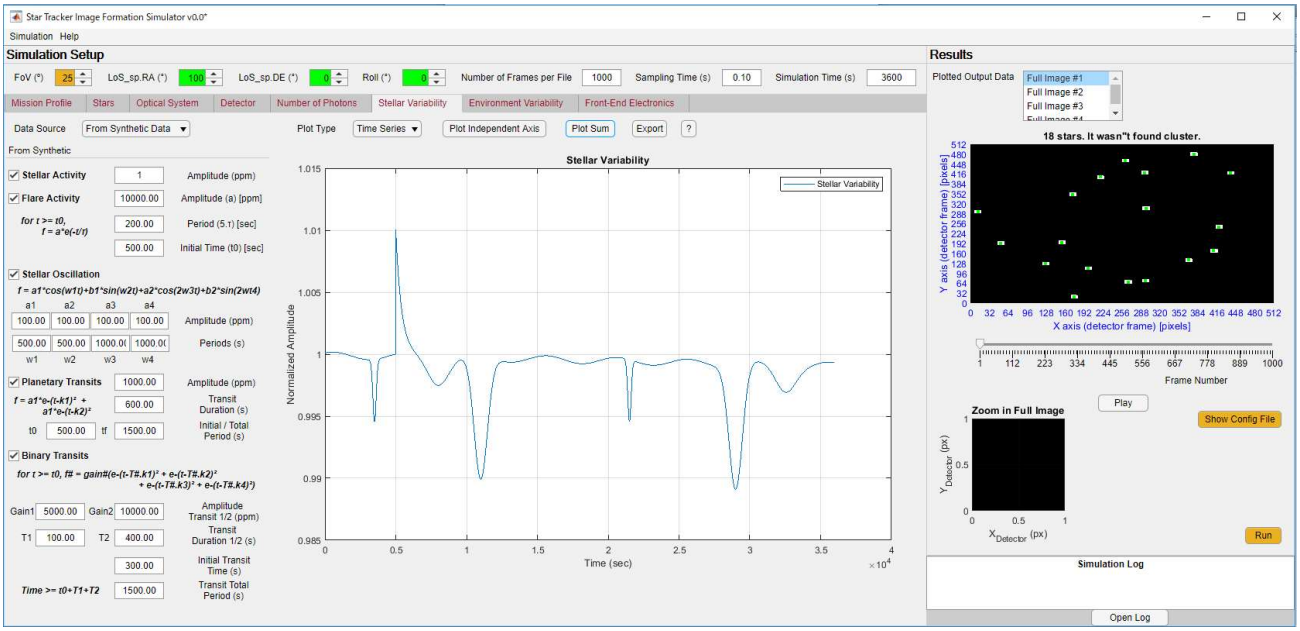

Figure 13- Human-machine interface of the star tracker image formation simulator.

6. DISCUSSIONS AND CONCLUSIONS

The present work has dealt with the development of a star tracker image formation simulator. Its basic blocks have been implemented as well as its HMI based on ongoing and past works of our team. This paper also presented the definition of simple algorithms to simulate the most representative stellar activity phenomena. The last ones being chosen through the exploitation of the Gaia and GCVS catalogues for magnitudes up to 7.

The fitted curves, although very simple and not representative of each possible type of stellar activity phenomena, are particularly useful in the context of star tracker flight software design, because they produce both rapid and high-level flux variations, which are in fact what matters to the flight software. Moreover, they do not require specialized knowledge in Astrophysics from engineers, simplifying the IFS, which is of great importance for the design of a star tracker, since from it, one can simulate several scenarios/missions, with several phenomena that are observed in real world and, thus, guaranteeing the robustness of its project, and in the last instance, increasing the ACS robustness.

7. REFERENCES

Burger, K. C. ; Camelo, P. S. ; Gouveia, G. P. ; De Oliveira Fialho, F., 2018. “Embedded Star Catalog For Autonomous Star Trackers”. *In: III IAA Latin American CubeSat Workshop*, Ubatuba, Brasil.

C. C. Liebe, 2002. “Accuracy performance of star trackers - a tutorial,” *IEEE Trans. Aerosp. Electron. Syst.*, vol. 38, no. 2, pp. 587–599.

Di Gennaro, Thiago M.; FIALHO, Fábio de Oliveira, 2016. “Algoritmo de cálculo do número de fótons detectados por uma câmera dedicada a observações astronômicas fotométricas em satélites: aplicação a um sensor estelar”. *Congresso Brasileiro de Automática 2016*, Vitória-ES, Brasil.

Gaia Collaboration, A. G. A. Brown, A. Vallenari, T. Prusti, J. H. J. de Bruijne, C. Babusiaux and C. A. L. Bailer-Jones, 2018b. *Gaia Data Release 2*. Summary of the contents and survey properties.

Rakesh R. Warier, Arpita Sinha, Srikant Sukumar, 2016. “Line-of-sight based spacecraft attitude and position tracking control”, *European Journal of Control*, Volume 32, Pages 43-53, ISSN 0947-3580.

Samus N.N., Kazarovets E. V., Durlevich O.V., Kireeva N.N., Pastukhova E.N., 2017. “General Catalogue of Variable Stars: Version GCVS 5.1”, *Astronomy Reports*, vol. 61, No. 1, pp. 80-88.

Vasily Belokurov, N. Wyn Evans, Yann Le Du, 2003. “Light-curve classification in massive variability surveys — I. Microlensing”, *Monthly Notices of the Royal Astronomical Society*, Volume 341, Issue 4, 1 June 2003, Pages 1373–1384, <https://doi.org/10.1046/j.1365-8711.2003.06512.x>.

8. RESPONSIBILITY NOTICE

The authors are the only responsible for the printed material included in this paper.